Active Flutter Suppression Using Trailing-Edge and Tab Control Surfaces

E. Nissim*
Technion – Israel Institute of Technology, Haifa, Israel

An optimization procedure, based on the aerodynamic energy concept, is applied to the problem of flutter suppression using trailing-edge (T.E.) and tab control surfaces. A control law is assumed which allows the T.E.-tab system to be driven by both linear and rotational sensors, and the optimum control law parameters are determined. Results are presented which indicate the capability of the T.E.-tab control system to suppress flutter. A comparison is also made between the T.E.-tab and the leading-edge (L.E.)-T.E. control systems which shows their relative effectiveness, together with some aspects connected to the realization of the control law.

Introduction

FLUTTER suppression using active controls has added, in recent years, a new potential for the design of light, flutter-free structures. It consists of a rapidly responding control system, which is activated by the motion of the main surface and which leads to an appropriate deflection of the control surface. The control surface thus activated gives rise to aerodynamic forces which are used to combat the flutter instability. It is, therefore, apparent that the effectiveness of an active control system in suppressing flutter is essentially dependent on the relationship between the motion of the main surface and the deflection of the control surface. This relationship is called the control law of the activated control system and is generally determined by applying various methods common in control system theory. It appears, however, that flutter suppression control systems (like mode stabilization control systems) show a great sensitivity to changes in flight conditions or flight configurations. This sensitivity implies that a control law determined, through some optimization procedure, to yield the highest flutter speed at a certain specified configuration, may prove to have a degraded performance at other flight configurations. This degradation in performance may lead to flutter speeds which are, at times, lower than those associated with the unactivated aircraft. The determination of a satisfactory control law which copes with the variety of flight configurations can, thus, be seen to be a difficult task, which requires a considerable amount of ingenuity from the control system designer.

The aerodynamic energy concept[1] forms an alternative approach to problems of flutter suppression using active controls. This latter approach is based on the fact that flutter instabilities are inherently connected to the nature of the aerodynamic forces acting on the main surfaces of the aircraft. These forces permit a transfer of energy from the surrounding airflow into the structure. The control surfaces can be effective in suppressing flutter at any flight configuration, provided the control surfaces can be activated so as to change the overall nature of the aerodynamic forces. This approach seems appropriate since it enables one to get to the roots of the flutter suppression problem.

Presented as Paper 75-822 at the AIAA/ASME/SAE 16th Structures, Structural Dynamics, and Materials Conference, Denver, Colo., May 27-29, 1975; submitted July 23, 1975; revision received Dec. 31, 1975. This work is part of a study supported by NASA under Grant NSG-7072.

Index category: Aeroelasticity and Hydroelasticity.

*Associate Professor. Now NRC-NASA Resident Research Associate, NASA Langley Research Center, Hampton, Va. Member AIAA.

Application of the aerodynamic energy concept[1] to flutter of a two-dimensional wing strip (using active controls) has shown that two independent control surfaces and two sensors are required for each such strip to insure complete flutter suppression. Reference 1 limited itself to the investigation of a single set of independent control surfaces, which included a leading-edge (L.E.) control and a T.E. control. The L.E. control may present some control problems[2] since it carries relatively large aerodynamic hinge moments. An alternative control surface, which could replace the L.E. control and lead to flutter suppression with reduced levels of control surface hinge moments, could alleviate these control problems. In the present work, a T.E.-tab control suface system is investigated in an attempt to determine both the effectiveness of the system and the values of the control parameters which insure best performance.

Optimization Parameters

Aerodynamic Energy Concept

Let the equations of motion of a system be given by

$$\{F\} = -\omega^2 [B + \pi\rho b^4 s(A_R + iA_I)]\{q\} + [E]\{q\} \quad (1)$$

where, at flutter

$$\{F\} = 0$$

and ω represents the frequency of oscillation; $[B]$, the mass matrix; $[A_R]$ and $[A_I]$, the real and imaginary parts of the aerodynamic matrix, respectively; $[E]$ the stiffness matrix.

As shown in Ref. 1, Appendix A, the work $\bar{P}$ done by the system on its surroundings per cycle can be written as

$$\bar{P} = \tfrac{1}{2}\pi^2\rho b^4 s\omega^2 \lfloor q_R - q_I \rfloor [-(A_I + A_I^T) + i(A_R - A_R^T)]\{q_R + iq_I\} \quad (2)$$

where

$$\{q\} = \{q_0\}e^{i\omega t} = \{q_R + iq_I\}e^{i\omega t} \quad (3)$$

Equation (2) can further be reduced to the following form:

$$\bar{P} = \tfrac{1}{2}\pi^2\rho b^4\omega^2 s[\lambda_1(\xi_{R1}^2 + \xi_{I1}^2) + \lambda_2(\xi_{R2}^2 + \xi_{I2}^2) + \cdots + \lambda_n(\xi_{Rn}^2 + \xi_{In}^2)] \quad (4)$$

where the λ_i's are the eigenvalues (necessarily real) of the Hermitian matrix

$$[U] = [-(A_I + A_I^T) + i(A_R - A_R^T)] \quad (5)$$

and where $\{\xi_R\}$ and $\{\xi_I\}$ are the generalized energy coordinates defined by

$$\{q_0\} = [Q_R + iQ_I]\{\xi_R + i\xi_I\} \tag{6}$$

The matrix $[Q_R + iQ_I]$ is the square modal matrix of the eignevectors of $[U]$.

Equation (4) shows that flutter cannot exist for any mode of oscillation (any $\{\xi_R\}$ and $\{\xi_I\}$), provided all the λ's are made positive. An attempt will, therefore, be made, during the process of optimization to increase the smallest λ to maximum, within the constraints of the control law.

Control Law

The matrix $[U]$ [Eq. (5)], which yields the aerodynamic eigenvalues λ_i, is a function of the reduced frequency k and Mach number M. Therefore, the changes made to $[U]$, through the activation of the control surfaces, will have to show some form of dependence on k and M. This latter dependence is inherent in the aerodynamic derivatives of the control surface deflections and can be extended, if necessary, to the control law itself.

Following Ref. 1, the following form of control law, which is independent of M, is suggested:

$$\begin{Bmatrix} \beta \\ \delta \end{Bmatrix} = ([C] + i[G]) \begin{Bmatrix} h/b \\ \alpha \end{Bmatrix} \tag{7}$$

where β is the T.E. control rotation and δ is the tab rotation (see Fig. 1) and $[C]$ and $[G]$ are the controlling matrices, which may depend on k, that is,

$$[C] = [C_0] + k[C_1] + k^2[C_2] + \cdots$$
$$[G] = [G_0] + k[G_1] + k^2[G_2] + \cdots \tag{8}$$

For the lower range of reduced frequencies, Eq. (8) can be represented by

$$[C] = [C_0] \quad [G] = [G_0] \tag{9}$$

The present work makes use of Eqs. (7) and (9) to represent the form of the control law.

For a two-dimensional system (applicable to wings through the use of the strip theory) $[A_R]$ and $[A_I]$ involve 2×2 matrices, yielding two eigenvalues designated as λ_{MIN} and λ_{MAX}. The matrices $[A_R]$ and $[A_I]$ of the basic two-dimensional strip are modified through the various C_{ij} and G_{ij} values to include the control surface contributions. The process of optimization allows the variation of the control law parameters (matrices $[C]$ and $[G]$), within a predetermined range of values, in a manner which insures maximum values for λ_{MIN}.

Physical Dimensions of Control Surfaces

The results of Ref. 1 have shown that the L.E. control is ineffective as regards the creation of lift forces. Its main effectiveness is based on its ability to provide out-of-phase pitching moments (i.e., damping-type moments) without appreciably affecting the lift forces. Extending these results to the T.E.-tab control system, the ratio $(\delta/\beta)_{L=0}$ of control surface rotaions which produces a zero net lift force is determined for various tab sizes (assuming 20% chord T.E. control, $M=0$ and $k=0$). The resulting pitching moment C_{MR} (normalized with respect to the pitching moment produced by a unit T.E. control rotation) and the pitching-moment derivative C_{MRC} (defined by $C_{MR}/(\delta/\beta)_{L=0}$) are presented in Table 1. It can be seen that the tab sizes in the range of 6-8% yield the largest values of C_{MRC} and are, therefore, the most efficient in controlling pitch. The 8% tab size was chosen for this investigation, since it was felt that the smaller tabs may be more severely affected by the existence of boundary layer. Hence, a 20% T.E. control and 8% tab control will be considered in the present investigation.

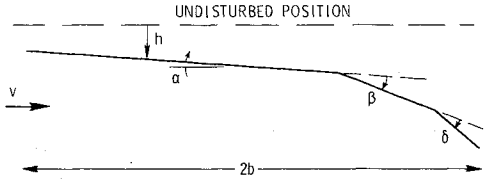

Fig. 1 Sketch of trailing-edge and tab control surfaces showing symbols used in study of flutter suppression.

Results

Optimization Results

In the following, the optimum control gains are presented and the sensitivity of these gains to changes around the optimum is examined. The peak power required to drive the control surfaces, at optimum, is estimated for a specific example. The effects of phase lags and amplitude gains, associated with control actuators, are evaluated and are followed by a discussion relating to an alternate control law. A comparison is also made between the results obtained for the T.E.-tab system and those relating to the L.E.-T.E. system (as presented in Ref. 1).

Optimization was carried out at two Mach numbers, that is, at $M=0$ and $M=0.9$. The results obtained yield the following values for the optimum control parameters (within their constrained range of variation) which relate to the movement of the 30% chord point:

For $M=0.9$

$$[C]_{opt} = \begin{bmatrix} 0.35 & -1.7 \\ 0.05 & 0 \end{bmatrix} \qquad [G]_{opt} = \begin{bmatrix} 0.50 & -1.0 \\ 0.50 & 2.0 \end{bmatrix}$$

For $M=0.9$

$$[C]_{opt} = \begin{bmatrix} -0.5 & -1.8 \\ 0 & -0.1 \end{bmatrix} \qquad [G]_{opt} = \begin{bmatrix} 0.50 & -1.0 \\ 0.40 & 2.1 \end{bmatrix}$$

Sensitivity of λ_{MIN} to off-design values around the optimum was made for each C_{ij} and G_{ij} parameter for both $M=0$ and $M=0.9$. The results indicate that the parameters C_{11}, C_{21}, C_{22}, G_{21} have little effect on λ_{MIN}, whereas the remaining parameters have a considerable effect. Figures 2-5 show some typical variations with off-design values of few control parameters at $M=0.9$.

The following remarks should be made regarding the optimization.

a) λ_{MIN} increases continuously with the simultaneous increase in both G_{12} and G_{21}. The value of G_{12} is, therefore, fixed at a chosen value while allowing the variation of all the other parameters during optimization.

b) The insensivity of G_{21} should be somewhat qualified so as to indicate that its insensitivity is dependent on the value of

Table 1 Variation with tab size of pitching moment of T.E.-tab system at $M=0$ and $k=0$

Tab chord (%)	$(\delta/\beta)_{L=0}$	C_{MR}	C_{MRC}
4	−2.17	−0.278	0.128
6	−1.78	−0.242	0.136
7	−1.65	−0.225	0.136
8	−1.54	−0.207	0.134
10	−1.39	−0.172	0.124
15	−1.14	−0.085	0.075

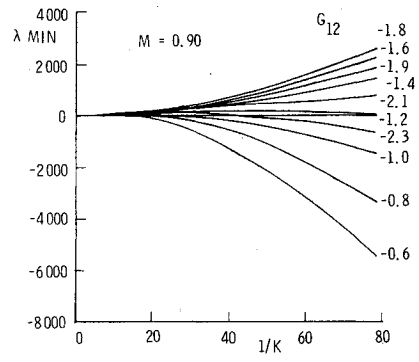

Fig. 2 Effects on λ_{MIN} of variation of C_{12} around its optimum value.

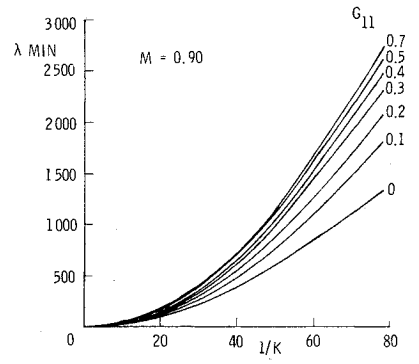

Fig. 3 Effects on λ_{MIN} of variation of G_{11} around its optimum value.

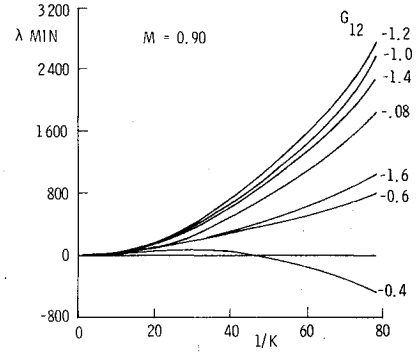

Fig. 4 Effects on λ_{MIN} of variation of G_{12} around its optimum value.

G_{11}. For large values of G_{11}, G_{21} shows a small sensitivity. This sensitivity, however, increases as G_{11} is made smaller.

Following the above sensitivity tests to off-design values, the following control parameters are determined as appropriate for both $M=0$ and $M=0.9$.

$$[C]_{opt}=\begin{bmatrix}0 & -1.7\\ 0 & 0\end{bmatrix} \qquad [G]_{opt}=\begin{bmatrix}0.5 & -1.0\\ 0 & 2.0\end{bmatrix}$$

Peak Power Requirements

Having determined the parameters of the control law, one can now proceed and evaluate, using the equations of motion, the forces which have to be exerted on the controls so as to realize the required control deflections. These forces are, in general, complex and, as a result, the power required to drive the controls will depend on both the response of the structure and the phase relationship between this response and the control forces. In an attempt to obtain some ideas regarding power requirements and the effect of the control law

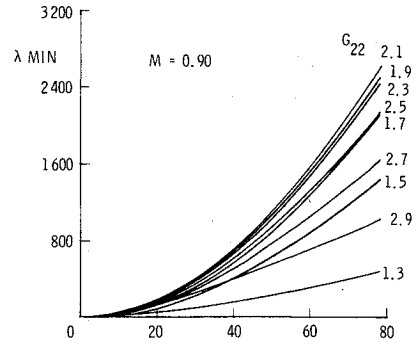

Fig. 5 Effects on λ_{MIN} of variation of G_{22} around its optimum value.

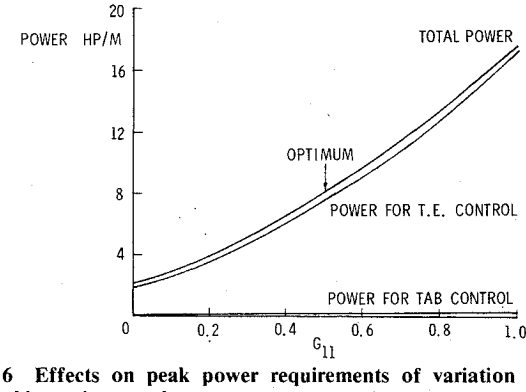

Fig. 6 Effects on peak power requirements of variation of G_{11} around its optimum value.

parameters on this power, it will be assumed that the phase relationship between the control forces and the response is such as to require maximum power. In this manner we effectively concentrate on peak power requirements. The resulting analysis is straightforward and follows the lines indicated in Ref. 1. The general data for the power estimate are similar to the data used in Ref. 1 for the case of the L.E.-T.E. system, and assume the following values: elastic matrix for control surface deflections equals zero; wing chord, 3.048 m (10 ft); velocity, 243.84 m/sec (800 fps); altitude, sea level; mass ratio 4; T.E. control, 20% chord; tab control, 8% chord; $|h_0/b|=0.2$; $|\alpha_0|=0.044$ rad $=2.5$ deg; $h_0=0.3048$ m $=1$ ft; $\omega=12$ rad/sec

$$[C]=\begin{bmatrix}0 & -1.7\\ 0 & 0\end{bmatrix} \qquad [G]=\begin{bmatrix}0.5 & -1.0\\ 0 & 2.0\end{bmatrix}$$

$$[B_C]=\begin{bmatrix}0.33942 & 0.42993 & 0.09051 & 0.01883\\ 0.05431 & 0.07313 & 0.01882 & 0.00579\end{bmatrix}$$

where h_0 and α_0 are defined by

$$h=h_0e^{i\omega t} \qquad \alpha=\alpha_0e^{i\omega t}$$

and where the inertia torques T_β, T_δ per unit span (in kg) are given by

$$\begin{Bmatrix}T_\beta\\ T_\delta\end{Bmatrix}=-\omega^2[B_C]\begin{Bmatrix}h/b\\ \alpha\\ \beta\\ \delta\end{Bmatrix}$$

The control surfaces are allowed inertia values appropriate to flat-plate-type controls.

The results obtained indicate that the peak power requirement is most sensitive to variations in G_{11} and G_{21}. Figure 6 illustrates the variation of power with G_{11}. Smaller sensitivity of power requirements is exhibited by the other

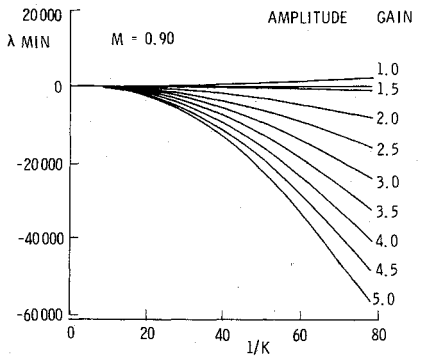

Fig. 7 Variation of λ_{MIN} with feedback amplitude gain using optimum values of C and G.

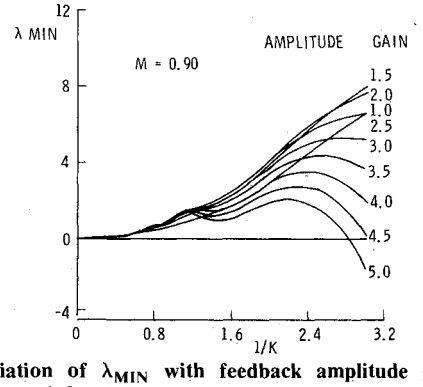

Fig. 8 Variation of λ_{MIN} with feedback amplitude gain using optimum values of C and G.

control parameters. It can be seen that the tab itself requires only a fraction of a hp/m for its activation. It has, however, a bigger effect on the power requirement of the T.E. control through its effect on the T.E. control aerodynamic hinge moments.

As regards the total power requirements, it has been shown[1] that the largest power requirement is expected at the lowest natural frequencies of the wing. Hence, the value of 8 hp/m span of the wing is not an unreasonably high one. Furthermore, the absolute values of the peak control deflections, as obtained from the optimum control law and response of the wing, are given by

$$\begin{Bmatrix} |\beta| \\ |\delta| \end{Bmatrix}_{\max} \cong \begin{Bmatrix} 0.19 \\ 0.09 \end{Bmatrix}$$

Therefore, the peak power requirements will not be excessive, even if we allow the peak control deflections to assume larger values, if necessary.

Phase Lag and Amplitude Effects of Activated Controls

The feedback control loop which activates the control surfaces forms, essentially, a second-order system. Therefore, phase lags and amplitude changes will be incurred between the desired and the actual control deflections. The sensitivity of the control system to these changes should, therefore, be investigated. Figures 7 and 8 show the effects of the amplitude gains at $M=0.9$. It can be seen that in the low-frequency range the system is very sensitive to amplitude gains. However, at the high-frequency range there is a marked reduction in the sensitivity of the system to amplitude gains. Similar results are obtained regarding the effects of the phase lag angles, as shown in Figs. 9 and 10. This indicates that the resonance frequency of the second-order system should be made high relative to the flutter frequencies, and that the damping coefficient of the system should assume relatively small values.

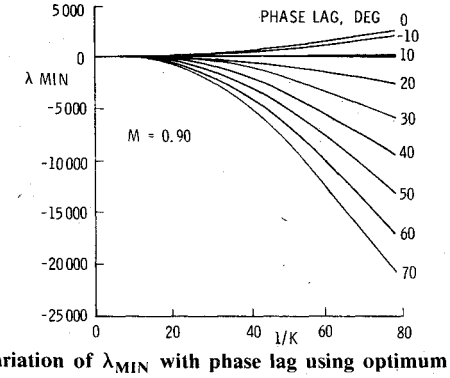

Fig. 9 Variation of λ_{MIN} with phase lag using optimum values of C and G.

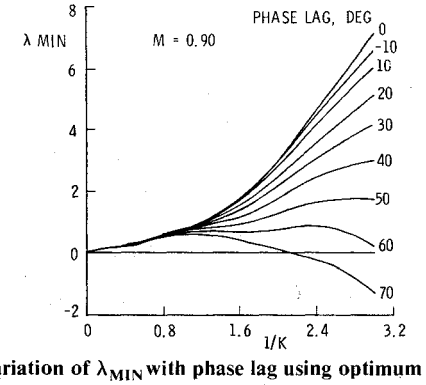

Fig. 10 Variation of λ_{MIN} with phase lag using optimum values of C and G.

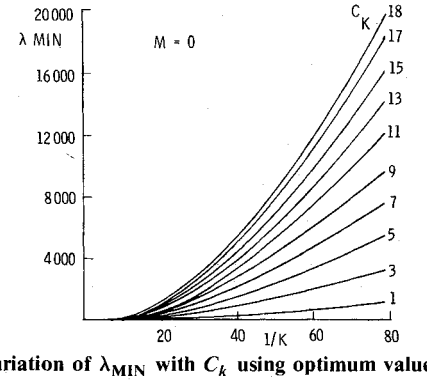

Fig. 11 Variation of λ_{MIN} with C_k using optimum values of C and G.

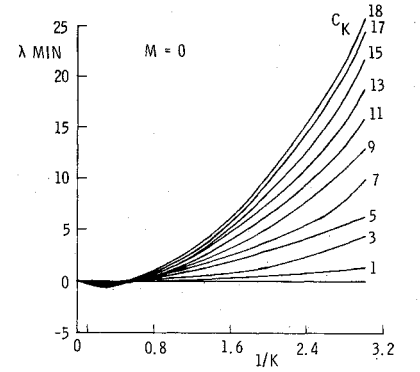

Fig. 12 Variation of λ_{MIN} with C_k using optimum values of C and G.

Alternate Control Law

The control law assumed in Eqs. (7) and (9) requires the determination of the frequency of oscillation to enable the 90° phase shift implied by the term $i[G]$. This phase shift is possible to achieve[2] but is not strictly necessary, as already remarked in Ref. 1. An indication to this effect in the present

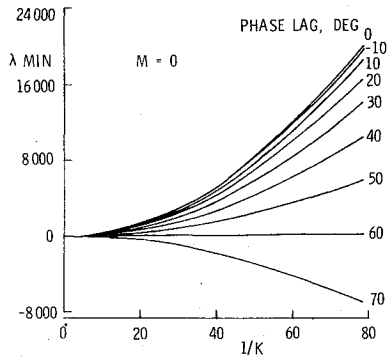

Fig. 13 Variation of λ_{MIN} with phase lag using optimum values of C and G, $C_k = 18$.

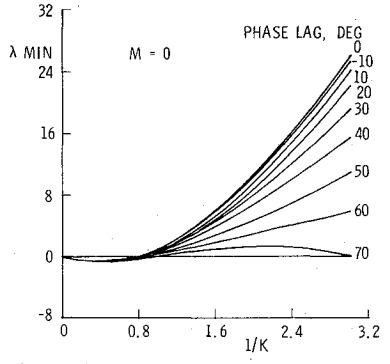

Fig. 14 Variation of λ_{MIN} with phase lag using optimum values of C and G, $C_k = 18$.

system is obtained by the necessity to fix the value of G_{12} during the process of optimization, as mentioned earlier in this work. It was, therefore, decided to investigate the effect of multiplying the matrix $[G]_{opt}$ by C_k, where C_k is allowed to vary between 1 and 18. Typical results for this variation are shown in Figs. 11 and 12 for $M=0$ (similar results are obtained for $M=0.9$). The effect of the phase lag angles for $C_k = 18$ is shown in Figs. 13 and 14 for $M=0$. It can be seen that the sensitivity of the system to phase lag angles is greatly reduced at high C_k values. From Eq. (8), the variation of λ_{MIN} with C_k can be incorporated into the control law by

$$\begin{Bmatrix} \beta \\ \delta \end{Bmatrix} = ([C_o] + ik[G_I]) \begin{Bmatrix} h/b \\ \alpha \end{Bmatrix} \tag{10}$$

Since

$$k = \omega b/V \tag{11}$$

Equation (10) can be written as

$$\begin{Bmatrix} \beta \\ \delta \end{Bmatrix} = [C_o] \begin{Bmatrix} h/b \\ \alpha \end{Bmatrix} + \frac{b}{V}[G_I] \begin{Bmatrix} \dot{h}/b \\ \dot{\alpha} \end{Bmatrix} \tag{12}$$

It is also possible to take an average value of b/V (over the flight speed range) and denote it as $1/\omega_r$ where ω_r has the dimensions of a frequency. Equation (12) can, therefore, assume the form suggested in Ref. 1.

$$\begin{Bmatrix} \beta \\ \delta \end{Bmatrix} = [C_o] \begin{Bmatrix} h/b \\ \alpha \end{Bmatrix} + \frac{1}{\omega_r}[G_I] \begin{Bmatrix} \dot{h}/b \\ \dot{\alpha} \end{Bmatrix} \tag{13}$$

The value of ω_r can be varied to insure reasonable values of control deflections. In general, the smaller ω_r is made, the more effective the activated controls become.

At this point attention should be drawn to the high-frequency range in Figs. 12 and 14 where λ_{MIN} assumes small negative values (only when C_k is large). This is not surprising since a control law was adopted which was assumed to operate at the low range of k values. It is, therefore, satisfying to note that, nevertheless, it produces satisfactory results, even at relatively high values of k (up to $k \simeq 2$), and with $C_k = 18$. The reason for the degradation of λ_{MIN} at the high k and C_k values lies in the changing nature of the aerodynamic forces at high frequencies. This change in the nature of the aerodynamic forces is not limited to control surface derivatives, as shown in Table 2.

The following notation relates to Table 2:

$$L = \pi\rho\omega^2 b^3 \Sigma L_r r, \quad (r = h, \alpha, \beta) \quad M_{c/4} = \pi\rho\omega^2 b^4 \Sigma M_r r$$

It can be clearly seen in Table 2 that both the lift and moment coefficients (due to T.E. control rotation) change their sign around $k \approx 4$, indicating the predominance of the aerodynamic inertia terms. This means that, for the range of high k values, the term $[C_2]$ from Eq. (8) should be incorporated into the control law, leading to a control law similar to the one formulated in Eq. (13), that is

$$\begin{Bmatrix} \beta \\ \alpha \end{Bmatrix} = [C_o] \begin{Bmatrix} h/b \\ \alpha \end{Bmatrix} + \frac{1}{\omega_{r1}}[G_1] \begin{Bmatrix} \dot{h}/b \\ \dot{\alpha} \end{Bmatrix} + \frac{1}{\omega_{r2}^2}[C_2] \begin{Bmatrix} \ddot{h}/b \\ \ddot{\alpha} \end{Bmatrix} \tag{14}$$

It is believed that Eq. (14) represents a control law capable of coping with a very wide range of k values. The values of the matrices $[C_0]$, $[G_1]$, $[C_2]$ can be determined by an optization procedure similar to the one used in this work. It is felt, however, that the testing of the extended control law is beyond the exploratory stage of the present work and is, therefore, deferred to a future extension of this work.

Comparison between L.E.-T.E. and T.E.-Tab Active Systems

It is very interesting to note the striking similarity between the L.E.-T.E. (from Ref. 1) and the T.E.-tab active systems. The similarity, in its general sense, is immediately apparent.

Table 2 Variation with k of aerodynamic derivatives at $M=0$ (βrelates to 20% chord T.E. control)

$1/k$	L_h	L_α	L_β	M_h	M_α	M_β
	1.0	0.5	0.02322	0.5	0.375	0.02126
0	0i	0i	0i	0i	0i	
	0.9848	0.42179	−0.01367	0.5	0.375	−0.0042
0.25	−0.2519i	−0.49423i	−0.06886i	0i	−0.25i	−0.06276i
	0.9423	0.18580	−0.12639	0.5	0.375	−0.0606
0.50	−0.5129i	−0.98405i	−0.13162i	0i	−0.50i	−0.12552i
	0.8538	−0.3823	−0.403]5	0.5	0.375	−0.26166
0.83	−0.8833i	−1.59487i	−0.18305i	0i	−0.8333i	−0.20919i
	0.7088	−1.5228	−0.97216	0.5	0.375	−0.61537
1.25	−1.3853i	−2.27119i	−0.18385i	0i	−1.250i	−0.3138i

However, to do justice to any quantitative comparisons they should be based on a chosen λ_{MIN} value, common to both systems. The L.E.-T.E. system yields a maximum λ_{MIN} value of about 1800 (at $M=0$, and $k^{-1}=78$) whereas the T.E.-tab system yields a corresponding value of about 1200. Figure 11 shows that λ_{MIN} varies almost linearly with C_k, implying that an approximate value of $C_k \approx 1.5$ applied to the T.E.-tab system should yield the required basis for comparison. With this in mind, one can find very little difference between the two system—even the peak power requirements are around the same values (12 hp/m vs 14 hp/m). Nevertheless, the following two major differences exist.

a) Peak control surface deflections: The optimum control law parameters associated with the L.E.-T.E. system are smaller than those associated with the T.E.-tab system, implying smaller control surface deflections for a given response. This can be seen from the following optimum control parameters. For the L.E.-T.E. system

$$\begin{Bmatrix} \text{L.E. control rotation} \\ \text{T.E. control rotation} \end{Bmatrix} = \left[\begin{bmatrix} 0 & 0 \\ 0 & -1.7 \end{bmatrix} + i \begin{bmatrix} 0 & 1.5 \\ 0.4 & 0.1 \end{bmatrix} \right] \begin{Bmatrix} h/b \\ \alpha \end{Bmatrix}$$

$$\begin{Bmatrix} \text{T.E. control rotation} \\ \text{tab rotation} \end{Bmatrix} = \left[\begin{bmatrix} 0 & -1.7 \\ 0 & 0 \end{bmatrix} + i \begin{bmatrix} 0.75 & -1.5 \\ 0 & 3.0 \end{bmatrix} \right] \begin{Bmatrix} h/b \\ \alpha \end{Bmatrix}$$

The peak control surface deflections are clearly limited, and on this basis the L.E.-T.E. system is superior. Furthermore, the tab control may operate within a fairly thick boundary layer, which may adversely affect its performance (note, however, that the T.E. rotation alleviates this problem to some extent).

b) Control surface hinge-moment levels: The similarity in peak power requirements between the two systems indicates that, at optimum, the hinge-moment levels during oscillation are of the same order. The largest differences between the two systems lie, however, in the hinge-moment levels which are brought about by changes made in the angle of attack α of the main surface. Table 3 shows the aerodynamic coefficients for very low k values (almost steady state) at $M=0$.

It can be seen that the L.E. control hinge-moment derivative with respect to α is about 23 times larger than the corresponding derivative associated with the T.E. control. These high hinge-moment levels introduce difficulties regarding actuator torque requirements and may greatly affect the peak power requirements if an initial value of α is assumed. The T.E.-tab system shows a considerable reduction in the hinge-moment levels leading to a comparable alleviation in actuator requirements and thus to an increase in actuator performance.

Table 3 Real part of aerodynamic derivatives for 20% chord L.E. control, 20% chord T.E. control, 8% chord tab at $M=0$, and $k=0.0128$

Aerodynamics derivatives (force/$\pi\rho\omega^2 b^4$)	Coordinate h/b	α	$\beta_{L.E.}$	$\beta_{T.E.}$	δ
Lift x b	−7	−11898	484	−6617	−4165
Moment (about 30% chord)	1	1190	−672	−1824	−1495
L.E. hinge moment	−1	−1770	413	−543	...
T.E. hinge moment	0	−76	−2	−139	−217
Tab hinge moment	0	−7	...	−12	−23

It is interesting to note that the optimum values of the control law parameters associated with the two control systems have an overall alleviating effect on the hinge-moment requirements.

Conclusions

The T.E.-tab system, activated by both linear and rotational sensors, is shown to have a flutter suppression performance comparable to the L.E.-T.E. active system. The main advantage of the T.E.-tab system over the L.E.-T.E. system lies in the lower actuator torque requirements, whereas its main disadvantage lies in its relatively higher control surface rotations. An extended alternate control law is suggested for future work relating to both control systems.

References

[1] Nissim, E., "Flutter Suppression Using Active Controls Based on the Concept of Aerodynamic Energy," NASA TN D-6199, March 1971.

[2] Sanford, M.C., Abel, I., and Gray, D.L., "Transonic Study of Active Flutter Suppression Based on an Aerodynamic Energy Concept," *Journal of Aircraft*, Vol. 12, Feb. 1975, pp. 72-77.